Inorg. Chem. **2008**, *47*, 9612−9623

Syntheses, Structures, and Properties of Copper(II) Complexes of Bis(2-pyridylmethyl) Derivatives of *o*-, *m*-, and *p*-Phenylenediamine and Aniline

Sabrina Turba,[†] Olaf Walter,[‡] Siegfried Schindler,*[,†] Lars Preuss Nielsen,[§] Alan Hazell,[||] Christine J. McKenzie,*[,§] Francesc Lloret,[⊥] Joan Cano,[⊥,#,○] and Miguel Julve*[,⊥]

Institut für Anorganische und Analytische Chemie, Justus-Liebig-Universität Giessen, Heinrich-Buff-Ring 58, 35392 Giessen, Germany, Institut für Technische Chemie−Chemisch-Physikalische Verfahren (ITC-CPV), Forschungszentrum Karlsruhe, Postfach 3640, 76021 Karlsruhe, Germany, Department of Physics and Chemistry, University of Southern Denmark, Campusvej 55, 5230 Odense M, Denmark, Department of Chemistry, Aarhus University, 8000 Aarhus, Denmark, Instituto de Ciencia Molecular (ICMol)/Departament de Química Inorgànica, Universitat de València, Polígono La Coma s/n, 46980 Paterna, València, Spain, Departament de Química Inorgànica, Institut de Química Teòrica i Computacional (IQTC), and Institució Catalana de Recerca i Estudis Avançats (ICREA), Universitat de Barcelona, diagonal 647, 08028 Barcelona, Spain

Received February 6, 2008

Copper(II) complexes of the ligand 1,*n*-bis[bis(2-pyridylmethyl)amino]benzene with $n = 2-4$ (1,*n*-tpbd) and its mononuclear derivative bis(2-pyridylmethyl)aniline (phbpa) were synthesized and structurally characterized. Magnetic measurements and DFT calculations were performed on $[CuCl_2(phbpa)]$, $[Cu_2Cl_4(1,3\text{-tpbd})]$, $[(Cu_2Cl_2(ClO_4)(1,3\text{-tpbd}))Cl(Cu_2Cl_2(OH_2)(1,3\text{-tpbd}))](ClO_4)_2$, and $[Cu_2(OH_2)_2(S_2O_6)(1,3\text{-tpbd})]S_2O_6$, and the exchange-polarization mechanism was successfully demonstrated.

Introduction

Parallel spin alignment (ferromagnetic coupling) in magnetic systems is not an easy task, and two main strategies are used to achieve it. These are based on either the orbital symmetry or the spin-polarization mechanism.[1−5] The first strategy requires the strict or accidental orthogonality between the interacting magnetic orbitals, and it has been illustrated by a good number of magneto-structural studies on heterobimetallic species[1,6] and meta-radical systems.[7] However, the second strategy has received less attention in the context of the metal complexes[8−15] when one looks at the extensive work that deals with the high-spin organic polyradicals.[16−18]

The series of ligands 1,*n*-bis[bis(2-pyridylmethyl)amino]benzene with $n = 2-4$ (see Scheme 1) appears to offer an opportunity for the testing of the spin-polarization mechanism for the magnetic exchange coupling in coordination compounds. With respect to this opportunity, in previous work, we have found that significant intramolecular magnetic interactions occur in the dicopper(II) complexes $[Cu_2(ClO_4)_3(OH_2)_2(1,3\text{-tpbd})]ClO_4$ (**1**) ($J = +9.3\,cm^{-1}$)[19] and $[Cu_2(OH_2)_4(1,4\text{-tpbd})](S_2O_6)_2$ (**2**) ($J = -15.6\ cm^{-1}$)[20] (see Scheme 2); the values of the intramolecular Cu···Cu distances are 5.873(1) and 8.259(4) Å, respectively.

The ferromagnetic coupling in complex **1** was successfully interpreted by the use of density functional theory (DFT)

* To whom correspondence should be addressed. E-mail: siegfried.schindler@chemie.uni-giessen.de (S.S), chk@ifk.sdu.dk (C.M.), miguel.julve@uv.es (M.J.).
[†] Justus-Liebig-Universität Giessen.
[‡] Forschungszentrum Karlsruhe.
[§] University of Southern Denmark.
[||] Aarhus University.
[⊥] Universitat de València.
[#] Departament de Química Inorgànica and Institut de Química Teòrica I Computacional (IQTC), Universitat de Barcelona.
[○] Institució Catalana de Recerca i Estudis Avançats (ICREA).

(1) Kahn, O. *Molecular Magnetism*; VCH: New York, 1993.
(2) McConnell, H. M. *J. Chem. Phys.* **1961**, *35*, 1520–1521.
(3) Mataga, N. *Theor. Chim. Acta* **1968**, *10*, 372–376.
(4) Kollmar, C.; Kahn, O. *Acc. Chem. Res.* **1993**, *26*, 259–265.
(5) Miller, J. S.; Epstein, A. J. *Angew. Chem., Int. Ed. Engl.* **1994**, *33*, 385–415.
(6) Kahn, O. *Adv. Inorg. Chem.* **1995**, *43*, 179–257.
(7) Caneschi, A.; Gatteschi, D.; Sessoli, R.; Rey, P. *Acc. Chem. Res.* **1989**, *22*, 392–398.
(8) Mitsubori, S.; Ishida, T.; Nogami, T.; Iwamura, H. *Chem. Lett.* **1994**, *23*, 285–288.

10.1021/ic800244g CCC: $40.75
Published on Web 09/18/2008

Scheme 1. Ligands phbpa and 1,*n*-tpbd ($n = 2-4$)

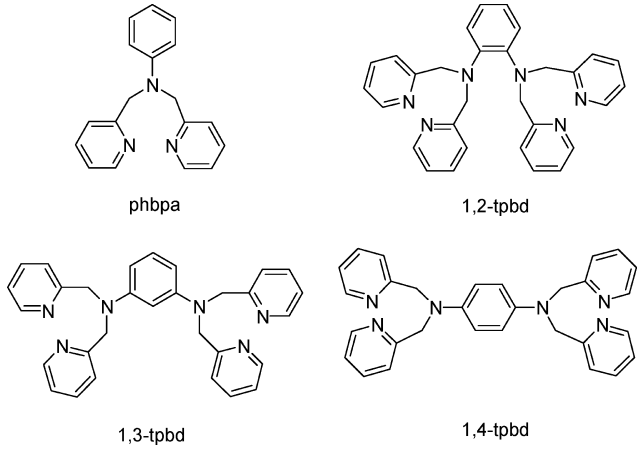

calculations,[19] and this finding is in good agreement with the properties of a related *N,N′*-1,3-phenylenebis(oxamate) dicopper(II) complex that also showed ferromagnetic coupling.[12] As illustrated by Scheme 2, the coordination spheres of the copper atoms in complexes **1** and **2** are not identical because a *O,O′*-perchlorate bridging group is present in complex **1** in addition to the phenylenediamine unit. However, no exchange pathway was associated with this perchlorate group in complex **1**, in contrast to what occurs with auxiliary bridges between the copper atoms in other dicopper(II) complexes of 1,3-tpbd, where they are found to be significant in the provision and the attenuation of magnetic exchange pathways.[19,21]

To elucidate whether the magnetic behavior of the dicopper(II) complexes of the geometrical isomers of tpbd follows the spin-polarization mechanism, we prepared several dinuclear copper(II) species with the ligands 1,3-tpbd and 1,4-tpbd. In principle, these complexes would contain copper(II) ions with chemically identical coordination spheres. Furthermore, we would prepare the unknown geometrically isomeric 1,2-tpbd ligand and its corresponding dicopper(II) compound. This latter species is expected to exhibit an antiferromagnetic interaction between the copper(II) centers as it did for the corresponding complex with the 1,4-tpbd ligand. Thus the target dinuclear systems should have the formulation $[Cu_2(1,n\text{-tpbd})L_x]$ with $n = 2-4$ and L being a terminal monodentate or a chelating ligand that does not furnish a secondary bridging group. We focused on the use of terminal water or chloride ligands given that some of these systems with 1,3-tpbd and 1,4-tpbd were available to us, although the series was incomplete. For example, the already known $[Cu_2(OH_2)_4(1,4\text{-tpbd})]^{4+}$ seemed to be an appropriate prototype. Copper(II) complexes of the monotopic ligand bis(2-pyridylmethyl)aniline and phbpa, such as $[CuCl_2(phbpa)]$ (**3**),[22–25] were useful for geometric, spectroscopic, and magnetic comparisons. In the present work, we report on the synthesis and structural and magnetic characterization of mono- and dinuclear copper(II) complexes of 1,*n*-tpbd ($n = 2-4$) and phbpa.

Results and Discussion

Ligand Syntheses. The ligand phbpa was synthesized without any problems according to a previously published procedure.[22] For the reaction of 2-(chloromethyl)pyridine with *meta*- and *para*-phenylenediamine, we have now optimized the syntheses in order to favor the formation and the isolation of the tetrasubstituted 1,3-tpbd and 1,4-tpbd ligands.

None of our attempts to prepare 1,2-tpbd by using reaction conditions similar to those used for the related 1,3-tpbd and 1,4-tpbd derivatives provided us with a pure sample of the tetrasubstituted ortho compound. It was always contaminated by the trisubstituted derivative *N,N,N′*-tri(2-pyridylmethyl)-benzene-1,2-diamine. The reactions were carried out under an inert atmosphere with careful control of the pH in a variety of solvents. In general, the reaction mixtures became dark red more rapidly than they did for the corresponding 1,3-tpbd and 1,4-tpbd derivatives. This color is probably an indication of the presence of an oxidized byproduct formed by radical formation in the *o*-phenylenediamine unit and by consequent side reactions for 1,4-tpbd. Notably, although Sato et al. also attempted the preparation of 1,2-tpbd, they succeeded in the isolation of only its trisubstituted derivative.[26] These authors suggested that the tetrasubstituted derivative is not formed for steric reasons. Our results contrast with this in that we were able to prepare a mixture that contained both the tri- and the tetrasubstituted products. However, we failed to separate them satisfactorily in a pure form by using the usual chromatographic techniques. In one preparation, 1,2-tpbd was successfully separated from the

(9) Oshio, H.; Ichida, H. *J. Phys. Chem.* **1995**, *99*, 3294–3302.
(10) Cargill Thompson, A. M. W.; Gatteschi, D.; McCleverty, J. A.; Navas, J. A.; Rentschler, E.; Ward, M. D. *Inorg. Chem.* **1996**, *35*, 2701–2703.
(11) Lloret, F.; De Munno, G.; Julve, M.; Cano, J.; Ruiz, R.; Caneschi, A. *Angew. Chem., Int. Ed.* **1998**, *37*, 135–138.
(12) Fernández, I.; Ruiz, R.; Faus, J.; Julve, M.; Lloret, F.; Cano, J.; Ottenwaelder, X.; Journaux, Y.; Muñoz, M. C. *Angew. Chem. Int. Ed.* **2001**, *40*, 3039–3042.
(13) Pardo, E.; Faus, J.; Julve, M.; Lloret, F.; Muñoz, C.; Cano, J.; Ottenwaelder, X.; Journaux, Y.; Carrasco, R.; Blay, G.; Fernandéz, I.; Ruiz-García, R. *J. Am. Chem. Soc.* **2003**, *125*, 10770–10771.
(14) Pardo, E.; Bernot, K.; Julve, M.; Lloret, F.; Cano, J.; Ruiz-García, R.; Delgado, F. S.; Ruiz-Pérez, C.; Ottenwaelder, X.; Journaux, Y. *Inorg. Chem.* **2004**, *43*, 2768–2770.
(15) Pardo, E.; Morales-Osorio, I.; Julve, M.; Lloret, F.; Cano, J.; Ruiz-García, R.; Pasán, J.; Ruiz-Pérez, C.; Ottenwaelder, X.; Journaux, Y. *Inorg. Chem.* **2004**, *43*, 7594–7596.
(16) Dougherty, D. A. *Acc. Chem. Res.* **1991**, *24*, 88–94.
(17) Iwamura, H.; Koga, N. *Acc. Chem. Res.* **1993**, *26*, 346–351.
(18) Rajca, A. *Chem. Rev.* **1994**, *94*, 871–893.
(19) Foxon, S. P.; Torres, G. R.; Walter, O.; Pedersen, J. Z.; Toftlund, H.; Hüber, M.; Falk, K.; Haase, W.; Cano, J.; Lloret, F.; Julve, M.; Schindler, S. *Eur. J. Inorg. Chem.* **2004**, 335–343.
(20) Buchen, T.; Hazell, A.; Jessen, L.; McKenzie, C. J.; Nielsen, L. P.; Pedersen, J. Z.; Schollmeyer, D. *Dalton Trans.* **1997**, 2697–2704.
(21) Foxon, S. P.; Walter, O.; Koch, R.; Rupp, H.; Müller, P.; Schindler, S. *Eur. J. Inorg. Chem.* **2004**, 344–348.
(22) Hazell, A.; McKenzie, C. J.; Nielsen, L. P. *Polyhedron* **2000**, *19*, 1333–1338.
(23) Nielsen, A.; Bond, A. D.; McKenzie, C. J. *Acta Crystallogr., Sect. E* **2005**, *61*, 478–480.
(24) Nielsen, A.; Veltzé, S.; Bond, A. D.; McKenzie, C. J. *Polyhedron* **2007**, *26*, 1649–1657.
(25) Ugozzoli, F.; Massera, C.; Manotti Lanfredi, A. M.; Marsich, N.; Camus, A. *Inorg. Chim. Acta* **2002**, *340*, 97–104.
(26) Sato, M.; Mori, Y.; Takeaki, I. *Synthesis* **1992**, 539–540.

Scheme 2. Dicopper(II) Units in Complexes **1** (left) and **2** (right)

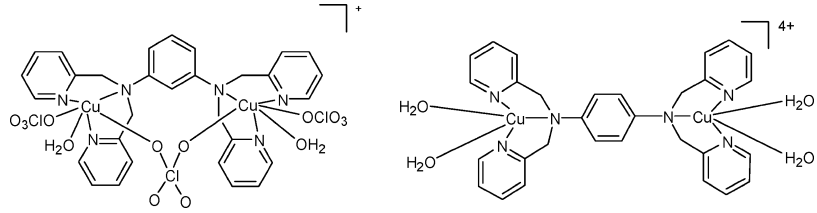

mixture via the isolation of the copper(II) complex [Cu(1,2-tpbd)]$(PF_6)_2$ (**4**), whose molecular structure is described below.

Copper(II) Complexes. Copper(II) complexes of all four ligands were isolated and characterized. Those described here are [$CuCl_2$(phbpa)] (**3**), [Cu(1,2-tpbd)]$(PF_6)_2$ (**4**), [Cu_2Cl_4(1,3-tpbd)]·0.84CH_3OH (**5**), [($Cu_2Cl_2(ClO_4)$(1,3-tpbd))Cl(Cu_2Cl_2-(OH_2)(1,3-tpbd))]$(ClO_4)_2$ (**6**), [$Cu_2(OH_2)_2(S_2O_6)$(1,3-tpbd)]-S_2O_6·2H_2O·CH_3OH (**7**), and [Cu_2Cl_4(1,4-tpbd)] (**8**). Compounds **3**, **5**, and **8** are lime green, whereas the complexes that include either water ligands or a combination of water and anion oxygen atoms in the copper environment are dark green.

[$CuCl_2$(phbpa)] (3). The crystal structure of compound **3** has been described previously;[25] however, because of the fact that different complexes can form when copper(II) salts react with phbpa,[24,25] we performed the reaction of phbpa with $CuCl_2$ under our conditions and crystallographically characterized the product. Its molecular structure is shown in Figure 1, and selected bond lengths and angles are listed in Table 2. The copper environment in compound **3** is an intermediate between square pyramidal and trigonal bipyramidal; the value of the trigonality parameter[27] is $\tau = 0.559$. ($\tau = (\beta - \alpha)/60$, where α and β are the two largest coordination angles around the five-coordinate copper atom; for ideal square-pyramidal geometry, $\tau = 0$, whereas for perfect trigonal-bipyramidal geometry, $\tau = 1$.) The three nitrogen atoms of the phbpa ligand and the copper atom are almost coplanar with $Cu-N_{py}$ bond distances of 1.988(2) and 1.997(2) Å, and $Cu-N_{amine} = 2.216(2)$ Å. They are all shorter than the Cu−Cl bond lengths (2.276(1) and 2.368(2) Å).

A closer inspection of the intermolecular interactions in compound **3** shows the presence of offset $\pi-\pi$-type interactions between adjacent pyridyl rings along the crystallographic *a* axis (shortest interplanar carbon−carbon distance of ca. 3.350 Å), which leads to a chain of weakly interacting mononuclear copper(II) units. (See Figure 2.)

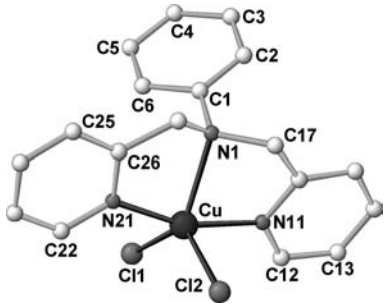

Figure 1. Molecular structure of [$CuCl_2$(phbpa)] (**3**). Hydrogen atoms are omitted for clarity.

[Cu(1,2-tpbd)]$(PF_6)_2$ (4). As expected, a mononuclear, rather than a dinuclear, copper(II) complex was obtained with the ortho-substituted ligand 1,2-tpbd. However, the addition of different copper(II) salts to mixtures of 1,2-tpbd and its trisubstituted derivative (see the Experimental Section) led to the isolation of several products. Very few crystals were obtained in one batch, and fortunately, they were suitable for X-ray diffraction. The molecular structure of compound **4** is shown in Figure 3. The structure contains two crystallographically independent copper atoms (Cu(1) and Cu(2)); the corresponding $[Cu(1,2\text{-tpbd})]^{2+}$ mononuclear cations are very similar. Their positive charge is neutralized by PF_6^- anions. Selected bond lengths and angles are listed in Table 2.

The coordination at the copper atoms is approximately trigonal bipyramidal, and N(2) and N(31) define the ternary axis. The value of the trigonality parameter τ is 0.728. The copper atoms are bonded to three pyridine nitrogen atoms and two amine nitrogen atoms, which leaves one pendant methylpyridine group that is uncoordinated. The $Cu-N_{py}$ lengths are in the range of 1.970(3)−2.102(3) Å, and the $Cu-N_{amine}$ lengths vary between 2.013(2) and 2.091(2) Å.

[Cu_2Cl_4(1,3-tpbd)]·0.84CH_3OH (5). The reaction of 1,3-tpbd with a stoichiometric amount of $CuCl_2$·2H_2O in a water/methanol mixture afforded X-ray-quality crystals of compound **5** as a methanol solvate. The structure of this compound, which is depicted in Figure 4, consists of discrete [Cu_2Cl_4(1,3-tpbd)] units and uncoordinated methanol molecules.

Selected bond lengths and angles for compound **5** are summarized in Table 2. The dinuclear unit contains two crystallographically independent copper atoms (Cu(1) and Cu(2)) that are linked via only the 1,3-phenylenediamine group, which causes an intramolecular Cu···Cu distance of 7.434(1) Å. The coordination geometry around Cu(1) is best described as distorted square pyramidal ($\tau = 0.335$) with N(11), N(21), N(1), and Cl(2) defining the basal plane and Cl(1) occupying the axial position. In contrast, the coordination around Cu(2) with $\tau = 0.535$ is intermediate between square pyramidal and trigonal bipyramidal. It could be viewed as a trigonal-bipyramidal coordination with the N(31) and N(41) atoms in the ternary axis (N(31)−Cu(2)−N(41) = 161.7(1)°). The three nitrogen atoms of the tridendate end of the 1,3-tpbd ligand and the copper atom to which they are bonded are almost coplanar; $Cu-N_{py}$ distances are in the range of 1.922(3)−2.003(4) Å, and $Cu-N_{amine}$ distances are 2.138(3) and 2.224(3) Å. The Cu−Cl distances are in the range of 2.276(1)−2.375(1) Å. The values of the C(6)−C(1)−N(1)−Cu(1) and C(6)−C(5)−N(2)−Cu(2) tor-

Table 1. Summary of Crystallographic Data for Compounds **3**, **4**, **5**·0.84CH_3OH and **6** and **7**·CH_3OH·$2H_2O$

compound	**3**	**4**	**5**·0.84CH_3OH	**6**	**7**·CH_3OH·$2H_2O$
formula	$C_{18}H_{17}N_3Cl_2Cu$	$C_{30}H_{28}N_6F_{12}P_2Cu$	$C_{30.84}H_{31.36}N_6O_{0.84}Cl_4Cu_2$	$C_{60}H_{56}Cl_8Cu_4N_{12}O_{13}$	$C_{31}H_{40}N_6O_{17}S_4Cu_2$
a (Å)	8.4065(8)	20.367(2)	8.6320(4)	8.2760(2)	8.5862(10)
b (Å)	14.133(1)	15.907(2)	27.471(1)	23.6354(4)	13.1174(2)
c (Å)	15.387(1)	22.082(2)	13.7959(7)	34.4974(5)	17.4616(3)
β (deg)	110.7730(6)	115.489(1)	93.007(1)	90	87.873(1)
V (Å^3)	1709.3(2)	6458(1)	3266.7(3)	6747.9(3)	1965.3(1)
Z	4	8	4	4	2
fw	409.80	826.07	768.41	1690.93	1024.05
space group	$P2_1/c$ (No. 14)	$P2_1/c$ (No. 14)	$P2_1/n$ (No. 14)	$P2_12_12_1$ (No. 19)	$P2_1$ (No. 4)
T (K)	294	120	295	200	200
λ (Å)	0.71073	0.71073	0.71073	0.71073	0.71073
ρ_{calcd} (g·cm^{-3})	1.592	1.699	1.562	1.664	1.730
μ (cm^{-1})	1.594	0.879	1.664	1.632	1.378
reflns collected	5877	82 374	22 243	71 148	20 197
reflns unique/R_{int}	4945/0.032	18 603/0.075	7912/0.048	16 345/0.0987	9305/0.016
data/restraints/params	3648/0/286[a]	10 429/0/920[a]	4095/11/408[a]	16 345/0/921[b]	8980/1/591[b]
R1, wR2	0.035/0.048[c]	0.039/0.044[c]	0.036/0.045[c]	0.0586/0.0916[d]	0.022/0.054[d]

[a] $I > 3\sigma(I)$ [b] $I > 2\sigma(I)$ [c] $w = 1/\{[\sigma(F_o^2) + 1.03(F_o^2)]^{1/2} - |F_o|\}^2$ [d] $w = 1/\{\sigma^2(F_o^2) + [0.0295(P)]^2 + 0.0474(P)\}$, where $P = (F_o^2 + 2F_c^2)/3$.

sion angles are 179.9 and 53.2°, respectively. Consequently, Cu(1) is within the plane of the bridging phenylene ring, whereas Cu(2) is well below this ring.

The crystal structures of compounds **3** and **5** reveal coordination geometries that are similar to those of the two complexes. However, the coordination sphere around the copper(II) core in compound **3** is very close to that of Cu(2) in compound **5**; the values of the trigonality parameter τ are practically identical (0.559 in compound **3** versus 0.535 for Cu(2) in compound **5**). The three nitrogen atoms and the copper(II) ion are almost coplanar at both cores.

Five-coordination around the copper atoms is also observed in the previously reported complex $[Cu_2(N_3)_4(1,3\text{-tpbd})]$,[21] where the azide groups act as terminal ligands. However, a less-distinctive distortion of the square-pyramidal geometry of Cu(2) occurs there. The Cu−N_{azide} distances in this complex are in the range 1.955(2)−1.979(2) Å and are remarkably shorter than the Cu−Cl distances in compound **5**. Interestingly, the two Cu−N_{amine} bonds in $[Cu_2(1,3\text{-tpbd})(N_3)_4]$ (2.474(2) and 2.138(2) Å for Cu(1)−N_{amine} and Cu(2)−N_{amine}, respectively) are significantly different; the shorter one is closer to the Cu−N_{amine} bond lengths in compound **5**. Finally, the Cu−N_{py} distances in $[Cu_2(1,3\text{-tpbd})(N_3)_4]$ vary in the range of 2.029(2)−2.176(2) Å, which stands in good agreement with the Cu−N_{py} distances in compound **5**.

$[(Cu_2Cl_2(ClO_4)(1,3\text{-tpbd}))Cl(Cu_2Cl_2(OH_2)(1,3\text{-tpbd}))](ClO_4)_2$ (6). A chloro-bridged tetracopper(II) compound (**6**) was isolated as a product when a mixture of perchlorate and chloride salts of copper(II) was used for the reaction with 1,3-tpbd. Its molecular structure is shown in Figure 5. This result lends support to an oligomeric/polymeric formulation in the case of compound **8**, as described below.

The structure of complex **6** consists of tetranuclear $[(Cu_2Cl_2(ClO_4)(1,3\text{-tpbd}))Cl(Cu_2Cl_2(OH_2)(1,3\text{-tpbd}))]^{2+}$ cations and uncoordinated ClO_4^- anions. Selected bond lengths and angles for this compound are given in Table 2. Four crystallographically independent copper atoms (Cu(1), Cu(2), Cu(3), and Cu(4)) occur in complex **6**. They are all five-coordinate. The environment at Cu(2), Cu(3), and Cu(4) is best described as distorted square pyramidal with values of τ ranging from 0.06 ((Cu(3)) to 0.22 (Cu(4)). The apical positions at Cu(2), Cu(3), and Cu(4) are filled by the Cl(1), O(61), and O(4) atoms, respectively, and the copper atoms are shifted by 0.152, 0.132, and 0.145 Å (Cu(4), Cu(2), and Cu(3), respectively) from the respective mean basal planes. Notably, Cu(1) has a significantly distorted coordination between square pyramidal and trigonal bipyramidal with a τ value of 0.520, which is most likely due to geometrical constraints. If it was described as trigonal bipyramidal, then the ternary axis would roughly correspond to the N(2)−Cu(1)−N(3) vector. The Cu−N_{amine} bond lengths of all of the four copper cores vary in the range 2.070(4)−2.143(4) Å (at Cu(3) and Cu(1), respectively), values that are somewhat longer than those concerning the Cu−N_{py} bond distances (1.985(4)−1996(4) Å). The values of the distances of copper to terminally bound chloro atoms cover the range 2.221(2)−2.310(2) Å; the longer value corresponds to the Cu(1)−Cl(2) bond (that is, to the copper with the greater τ value). These values are all shorter than those concerning the single chloro bridge (2.412(2) and 2.741(2) Å for Cu(1)−Cl(1) and Cu(2)−Cl(1), respectively), as expected because of the bridging role of Cl(1). The value of the angle at the chloro bridge and that of the corresponding copper−copper separation are 141.6(1)° and 4.868(1) Å. This last value is significantly shorter than the other intramolecular copper−copper separations through the bridging 1,3-tpbd ligand (7.121(1) and 6.183(1) Å for Cu(1)···Cu(3) and Cu(2)···Cu(4), respectively). The peripheral Cu−O bond distances are 2.322(4) and 2.371(4) Å for Cu(4)−O(4) and Cu(3)−O(61), respectively. The shortest intermolecular copper−copper separation is 6.503(1) Å. This is the intermolecular Cu(4)−Cu(4a) distance between two molecules that are symmetrically related by a double-screw-fold axis (symmetry code: $x + 0.5$, $0.5 - y$, $-z$); the two molecules are connected via an H bond between the terminal chloro ligand Cl(4) of one molecule and the terminal water molecule located at O(4a) (O(4a)···Cl(4) distance of 3.260(2) Å with a Cu(4a)−O(4a)−Cl(4) bonding angle of 115.8(2)°).

(27) Addison, A. W.; Rao, T. N.; Reedijk, J.; van Rijn, J.; Verschoor, G. C. *Dalton Trans.* **1984**, 1349–1356.

Table 2. Selected Bond Distances (Angstroms) and Angles (Degrees) for Compounds **3**, **4**, **5**·0.84CH_3OH and **6** and **7**·CH_3OH·$2H_2O$

atoms	**3**	atoms	**4**	atoms	**5**·0.84 CH_3OH	atoms	**6**	atoms	**7**·CH_3OH ·$2H_2O$
Cu−Cl(1)	2.276(1)	Cu(1)−N(1)	2.091(2)	Cu(1)−Cu(2)	7.434(1)	Cu(1)−N(2)	1.985(4)	Cu(1)−Cu(2)	5.763(2)
Cu−Cl(2)	2.368(1)	Cu(1)−N(2)	2.013(2)	Cu(1)−Cl(1)	2.370(1)	Cu(1)−N(3)	1.993(4)	Cu(1)−N(3)	1.971(2)
Cu−N(1)	2.216(2)	Cu(1)−N(11)	2.054(3)	Cu(1)−Cl(2)	2.295(1)	Cu(1)−N(1)	2.143(4)	Cu(1)−N(1)	1.974(2)
Cu−N(11)	1.988(2)	Cu(1)−N(21)	2.102(3)	Cu(1)−N(1)	2.138(3)	Cu(1)−Cl(2)	2.310(2)	Cu(1)−O(13)	1.992(2)
Cu−N(21)	1.997(2)	Cu(1)−N(31)	1.970(3)	Cu(1)−N(11)	1.993(4)	Cu(1)−Cl(1)	2.412(2)	Cu(1)−N(2)	2.091(2)
		Cu(1A)−N(1A)	2.088(2)	Cu(1)−N(21)	2.003(4)	Cu(2)−N(8)	1.988(4)	Cu(1)−O(2)	2.275(2)
		Cu(1A)−N(2A)	2.022(2)	Cu(2)−Cl(3)	2.276(1)	Cu(2)−N(9)	1.994(4)	Cu(1)−O(8)	2.444(6)
		Cu(1A)−N(11A)	2.039(3)	Cu(2)−Cl(4)	2.375(1)	Cu(2)−N(7)	2.083(4)	Cu(2)−N(4)	1.970(2)
		Cu(1A)−N(21A)	2.098(2)	Cu(2)−N(2)	2.224(3)	Cu(2)−Cl(3)	2.230(2)	Cu(2)−N(6)	1.972(2)
		Cu(1A)−N(31A)	1.979(3)	Cu(2)−N(31)	1.997(4)	Cu(2)−Cl(1)	2.741(2)	Cu(2)−O(14)	1.994(2)
				Cu(2)−N(41)	1.992(3)	Cu(3)−N(6)	1.986(5)	Cu(2)−N(5)	2.110(2)
						Cu(3)−N(5)	1.993(4)	Cu(2)−O(1)	2.342(2)
						Cu(3)−N(4)	2.070(4)	Cu(2)−O(9A)	2.967(4)
						Cu(3)−Cl(5)	2.221(2)		
						Cu(3)−O(61)	2.371(4)		
						Cu(4)−N(12)	1.991(4)		
						Cu(4)−N(11)	1.996(4)		
						Cu(4)−N(10)	2.087(4)		
						Cu(4)−Cl(4)	2.245(2)		
						Cu(4)−O(4)	2.322(4)		
Cl(1)−Cu−Cl(2)	123.91(3)	N(1)−Cu(1)−N(2)	84.8(1)	Cl(1)−Cu(1)−Cl(2)	115.1(1)	N(2)−Cu(1)−N(3)	161.7(2)	N(3)−Cu(1)−N(1)	164.95(7)
Cl(1)−Cu−N(1)	127.55(6)	N(1)−Cu(1)−N(11)	127.7(1)	Cl(1)−Cu(1)−N(1)	103.8(1)	N(2)−Cu(1)−N(1)	80.6(2)	N(3)−Cu(1)−O(13)	94.10(7)
Cl(1)−Cu−N(11)	96.43(6)	N(1)−Cu(1)−N(21)	106.7(1)	Cl(1)−Cu(1)−N(11)	92.4(1)	N(3)−Cu(1)−N(1)	81.3(2)	N(1)−Cu(1)−O(13)	98.63(7)
Cl(1)−Cu−N(21)	95.28(6)	N(1)−Cu(1)−N(31)	83.9(1)	Cl(1)−Cu(1)−N(21)	95.7(1)	N(2)−Cu(1)−Cl(2)	96.5(2)	N(3)−Cu(1)−N(2)	83.46(6)
Cl(2)−Cu−N(1)	108.52(6)	N(2)−Cu(1)−N(11)	82.5(1)	Cl(2)−Cu(1)−N(1)	141.1(1)	N(3)−Cu(1)−Cl(2)	97.1(2)	N(1)−Cu(1)−N(2)	82.97(6)
Cl(2)−Cu−N(11)	91.32(6)	N(2)−Cu(1)−N(21)	81.4(1)	Cl(2)−Cu(1)−N(11)	96.8(1)	N(1)−Cu(1)−Cl(2)	130.5(2)	O(13)−Cu(1)−N(2)	173.03(7)
Cl(2)−Cu−N(21)	94.35(6)	N(2)−Cu(1)−N(31)	164.7(1)	Cl(2)−Cu(1)−N(21)	95.1(1)	N(2)−Cu(1)−Cl(1)	94.0(2)	N(3)−Cu(1)−O(2)	101.47(7)
N(1)−Cu−N(11)	79.97(8)	N(11)−Cu(1)−N(21)	121.0(1)	N(1)−Cu(1)−N(11)	81.2(1)	N(3)−Cu(1)−Cl(1)	92.9(2)	N(1)−Cu(1)−O(2)	86.93(6)
N(1)−Cu−N(21)	81.17(8)	N(11)−Cu(1)−N(31)	112.6(1)	N(1)−Cu(1)−N(21)	80.5(1)	N(1)−Cu(1)−Cl(1)	120.4(2)	O(13)−Cu(1)−O(2)	88.55(6)
N(11)−Cu−N(21)	161.14(9)	N(21)−Cu(1)−N(31)	91.9(1)	N(11)−Cu(1)−N(21)	161.2(1)	Cl(2)−Cu(1)−Cl(1)	109.1(1)	N(2)−Cu(1)−O(2)	98.33(6)
		N(1A)−Cu(1A)−N(2A)	84.5(1)	Cl(3)−Cu(2)−Cl(4)	129.6(1)	N(8)−Cu(2)−N(9)	164.5(2)	O(2)−Cu(1)−O(8)	166.95(5)
		N(1A)−Cu(1A)−N(11A)	127.4(1)	Cl(3)−Cu(2)−N(2)	124.5(1)	N(8)−Cu(2)−N(7)	82.5(2)	N(1)−Cu(1)−O(8)	83.25(5)
		N(1A)−Cu(1A)−N(21A)	110.1(1)	Cl(3)−Cu(2)−N(31)	95.2(1)	N(9)−Cu(2)−N(7)	83.2(2)	N(2)−Cu(1)−O(8)	89.01(5)
		N(1A)−Cu(1A)−N(31A)	83.3(1)	Cl(3)−Cu(2)−N(41)	95.7(1)	N(8)−Cu(2)−Cl(3)	98.0(2)	N(3)−Cu(1)−O(8)	90.04(5)
		N(2A)−Cu(1A)−N(11A)	82.7(1)	Cl(4)−Cu(2)−N(2)	105.9(1)	N(9)−Cu(2)−Cl(3)	97.5(2)	O(13)−Cu(1)−O(8)	84.46(5)
		N(2A)−Cu(1A)−N(21A)	81.7(1)	Cl(4)−Cu(2)−N(31)	92.6(1)	N(7)−Cu(2)−Cl(3)	157.3(2)	N(4)−Cu(2)−N(6)	162.20(7)
		N(2A)−Cu(1A)−N(31A)	164.4(1)	Cl(4)−Cu(2)−N(41)	91.7(1)	N(8)−Cu(2)−Cl(1)	85.5(2)	N(4)−Cu(2)−O(14)	96.21(7)
		N(11A)−Cu(1A)−N(21A)	118.0(1)	N(2)−Cu(2)−N(31)	80.3(1)	N(9)−Cu(2)−Cl(1)	90.1(2)	N(6)−Cu(2)−O(14)	93.09(7)
		N(11A)−Cu(1A)−N(31A)	112.5(1)	N(2)−Cu(2)−N(41)	81.4(1)	N(7)−Cu(2)−Cl(1)	95.3(2)	N(4)−Cu(2)−N(5)	83.29(6)
		N(21A)−Cu(1A)−N(31A)	93.4(1)	N(31)−Cu(2)−N(41)	161.7(1)	Cl(3)−Cu(2)−Cl(1)	107.4(1)	N(6)−Cu(2)−N(5)	83.91(7)
						N(6)−Cu(3)−N(5)	162.8(2)	O(14)−Cu(2)−N(5)	165.43(7)
						N(6)−Cu(3)−N(4)	81.6(2)	N(4)−Cu(2)−O(1)	97.68(6)
						N(5)−Cu(3)−N(4)	81.3(2)	N(6)−Cu(2)−O(1)	98.26(6)
						N(6)−Cu(3)−Cl(5)	97.3(2)	O(14)−Cu(2)−O(1)	84.72(7)
						N(5)−Cu(3)−Cl(5)	98.7(2)	N(5)−Cu(2)−O(1)	109.80(6)
						N(4)−Cu(3)−Cl(5)	166.6(2)	O(1)−Cu(2)−O(9A)	161.98(5)
						N(6)−Cu(3)−O(61)	103.5(2)	N(4)−Cu(2)−O(9A)	76.29(5)
						N(5)−Cu(3)−O(61)	80.9(2)	N(5)−Cu(2)−O(9A)	86.60(5)
						N(4)−Cu(3)−O(61)	96.1(2)	N(6)−Cu(2)−O(9A)	90.65(5)
						Cl(5)−Cu(3)−O(61)	97.2(2)	O(14)−Cu(2)−O(9A)	79.17(5)
						N(12)−Cu(4)−N(11)	163.2(2)		
						N(12)−Cu(4)−N(10)	83.8(2)		
						N(11)−Cu(4)−N(10)	81.5(2)		
						N(12)−Cu(4)−Cl(4)	98.4(2)		
						N(11)−Cu(4)−Cl(4)	98.3(2)		
						N(10)−Cu(4)−Cl(4)	156.5(2)		
						N(12)−Cu(4)−O(4)	85.3(2)		
						N(11)−Cu(4)−O(4)	88.6(2)		
						N(10)−Cu(4)−O(4)	97.3(2)		
						Cl(4)−Cu(4)−O(4)	106.2(2)		

Chloride-bridged crystal structures, such as the one observed for complex **6**, were also reported for monotopic copper(II) complexes with the ligand phbpa. Ugozzoli et al. described the complex $[Cu_2Cl_3(phbpa)_2]PF_6 \cdot 0.5CH_3OH$.[25] The reported Cu−Cl bond distances at the chloro bridge in this compound are 2.568(2) and 2.504(2) Å, and the angle at the chloro bridge is 159.9(1)°; the differences observed with the respective values in complex **6** are most likely due to the presence in **6** of sterically demanding coordinated perchlorate groups. Nielsen et al. described the complex $[Cu_2Cl_2(CH_3CO_2)(phbpa)_2]PF_6 \cdot 1.5CH_3OH$, where in contrast with the complex reported by Ugozzoli, one chloro ligand is replaced by an acetate group.[24] Nevertheless, the values of the Cu−Cl bond distances and the Cu(x)−Cl−Cu(y) bond angle agree with Ugozzoli's earlier-described results.

$[Cu_2(OH_2)_2(S_2O_6)(1,3\text{-tpbd})]S_2O_6 \cdot 2H_2O \cdot CH_3OH$ (7). The dithionate copper complex with the 1,3-tpbd ligand (complex **7**) was prepared with the hope that a compound that was structurally isomeric to the previously reported complex **2** (i.e., an uncoordinated dithionate; this dianion acting exclusively as a counterion) would be obtained.[20] Compound **7** shows structural similarities to compound **1**. The structure of compound **7** consists of $[Cu_2(OH_2)_2(S_2O_6)(1,3\text{-tpbd})]^{2+}$ cations (Figure 6), $S_2O_6^{2-}$ anions, water molecules of crystallization,

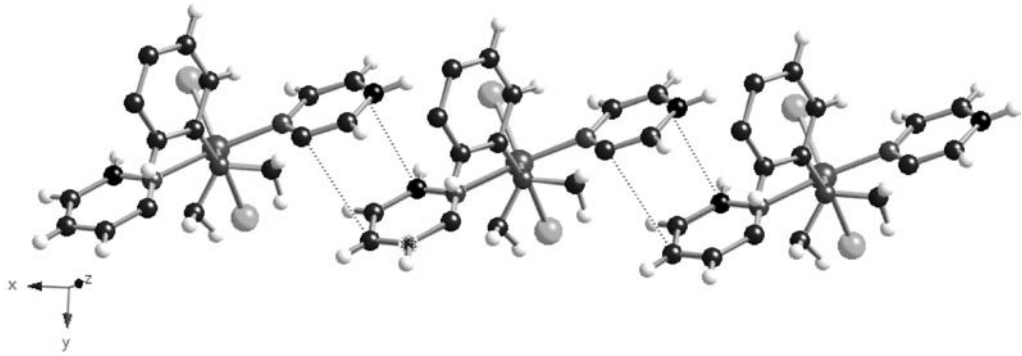

Figure 2. View of the chain formation in compound **3** through $\pi-\pi$-type interactions (dotted lines) along the *a* axis.

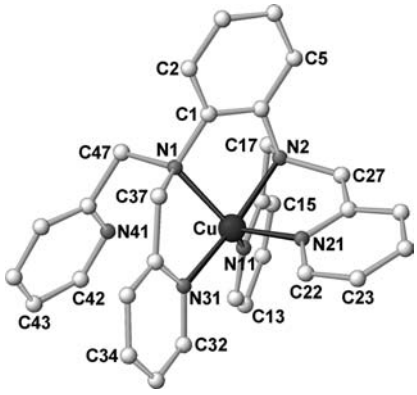

Figure 3. Molecular structure of the cation of $[Cu(1,2\text{-tpbd})](PF_6)_2$ (**4**). Hydrogen atoms are omitted for clarity.

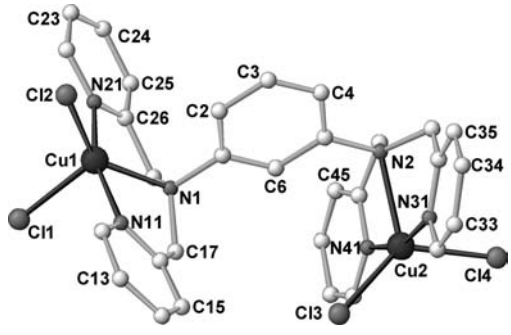

Figure 4. Molecular structure of $[Cu_2Cl_4(1,3\text{-tpbd})]\cdot 0.84CH_3OH$ (**5**) showing the atom numbering. Hydrogen atoms are omitted for clarity.

and a noncoordinated methanol molecule that is disordered over two sites with the oxygen position common to both molecules. Selected bond lengths and angles for compound **7** are listed in Table 2. The environment of the two crystallographically independent copper atoms (Cu(1) and Cu(2)) is close to square pyramidal with $\tau = 0.130$. The dithionate oxygen atoms O(2) and O(1), at Cu(1)and Cu(2), respectively, fill the axial positions, whereas a water molecule and three nitrogen atoms (one amine and two pyridyl atoms) occupy the equatorial positions at each copper atom. The two copper atoms are linked by a bis-tridentate 1,3-tpbd ligand and a bis-monodentate dithionate group. The intramolecular copper···copper distance is 5.736(1) Å, a value that is in this case shorter than the shortest intermolecular metal−metal separation (7.4317(1) Å for Cu(1)···Cu(2a)). The two molecules involved in this interaction are generated by a translation along the *b* axis that corresponds basically to the main orientation axis of an entire unit. Therefore, the resulting intermolecular distance of 7.4317(1) Å between Cu(1) and Cu(2a) can be estimated from the value of the *b* axis (13.1174 Å) that is diminished by the intramolecular Cu(1)−Cu(2) distance of 5.7361(1) Å. Therefore the view depicted in Figure 6 can be regarded as a view that is perpendicular to the *b* axis, which nicely shows the intermolecular connection of the moieties. The $Cu-N_{py}$ bond lengths cover the range of 1.970(2)−1.972(2) Å, values that are shorter than the $Cu-N_{amine}$ distances (2.091(2) and 2.110(2) Å). The $Cu-O_{water}$ distances are 1.992(2) and 1.994(2) Å, which are considerably shorter than those to the apical oxygen atoms provided by the bridging dithionate ($Cu-O_{dithionate} = 2.275(2)$ and 2.342(2) Å). The $Cu-O_{dithionate}$ distances to the nonbridging dithionate anions are 2.444(6) and 2.967(4) Å (for Cu(1)−O(8) and Cu(2)−O(9A), respectively), which are small enough to at least provide electronic interactions. The values of the torsion angles Cu(1)−N(2)−C(13)−C(14) and Cu(2)−N(5)−C(15)−C(14) are 81.570 and −76.661°, respectively. This indicates that the value in which both copper(II) ions are standing twisted to the bridging phenylene system is similar. They are standing nearly vertically to the aromatic system with a slightly parallel alignment. (The torsion angle Cu(2)−N(5)−N(2)−Cu(1) has a value of 11.947°.) The angle between the mean basal planes (Cu(1)−N(1)−N(2)−N(3)) and (Cu(2)−N(4)−N(5)−N(6)) is 126.7°. The copper(II) deviations of these planes are −0.076 and −0.144 Å for Cu(1) and Cu(2), respectively.

$[Cu_2Cl_4(1,4\text{-tpbd})]$ (8). The reaction of copper(II) chloride with 1,4-tpbd yields compound **8** as a very finely divided microcrystalline solid, and despite our numerous attempts, X-ray-suitable crystals of this material could not been obtained. The formula of compound **8** on the basis of the elemental analysis $[Cu_2Cl_4(1,4\text{-tpbd})]$ represents only the stoichiometry of the compound, and it is not necessarily the molecular unit. For example, a polynuclear compound with chloro bridges between the copper atoms cannot be excluded. Indeed, the structure of compound **6** shows one mode of chloro bridging that could occur in compound **8**.

Magnetic Properties. Results of previous magnetic studies on copper(II) complexes of 1,3-tpbd and 1,4-tpbd were discussed in the Introduction. Our efforts to prepare copper(II) complexes of all ligands with identical anions led to the isolation of compounds **3**, **5**, and **8**. Unfortunately, we could not obtain X-ray-quality crystals of compound **8** because this compound seems to form a very insoluble polymer. Because of the lack of structural characterization of compound **8** and the small amount of crystals of

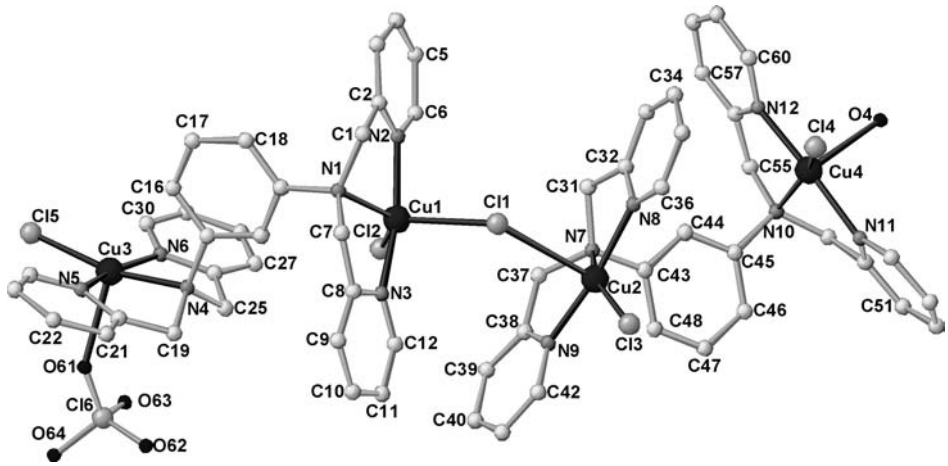

Figure 5. Molecular structure of the cation of $[(Cu_2Cl_2(ClO_4)(1,3\text{-tpbd}))Cl(Cu_2Cl_2(OH_2)(1,3\text{-tpbd}))](ClO_4)_2$ (**6**) with the atom numbering. Hydrogen atoms are omitted for clarity.

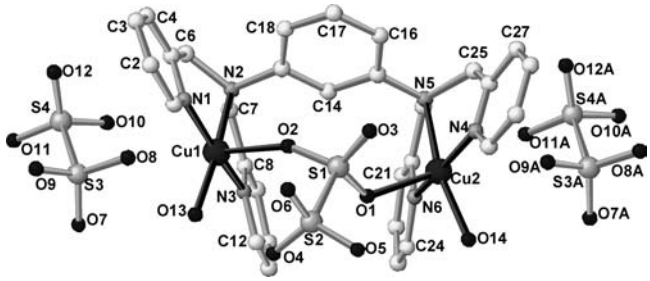

Figure 6. Molecular structure of $[Cu_2(OH_2)_2(S_2O_6)(1,3\text{-tpbd})]S_2O_6$ (**7**). One dithionate anion of the next asymmetric unit is shown. Hydrogen atoms are omitted for clarity.

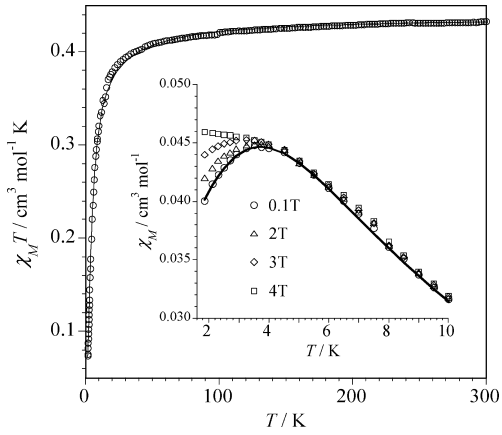

Figure 7. Thermal variation of $\chi_M T$ for compound **3** in an applied magnetic field of 0.1 T including experimental data (○) and a best-fit curve (—) through eq 1. (See the text.) The inset shows the maximum of the magnetic susceptibility in the low-temperature region.

compound **4** together with its mononuclear nature, the magnetic properties of these two compounds were not investigated.

Magnetic susceptibility measurements were carried out on polycrystalline samples of the structurally characterized complexes **3** and **5**−**7** in the temperature range of 1.9−300 K. The magnetic properties of compound **3** in the form of a $\chi_M T$ versus T plot (χ_M is the magnetic susceptibility per one copper(II) ion) are shown in Figure 7. At room temperature, $\chi_M T$ is equal to 0.420 cm^3 mol^{-1} K, a value that is as expected for two magnetically isolated spin doublets. Upon cooling, this value remains constant until $T = 50$ K, and it

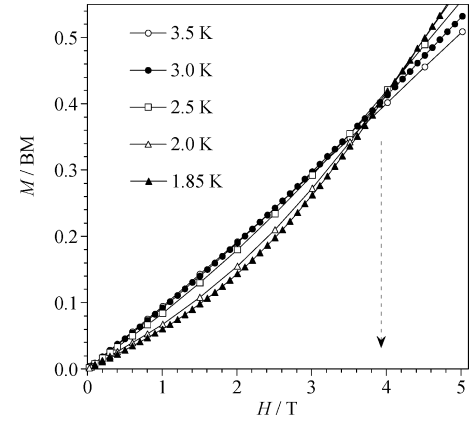

Figure 8. Magnetization versus H plot for compound **3** at $T = 1.85$, 2.0, 2.5, 3.0, and 3.5 K.

further decreases sharply to 0.050 cm^3 mol^{-1} K at 1.9 K. The susceptibility versus T plot (see inset of Figure 7) exhibits a maximum at ca. 3.7 K. These features are characteristic of a weak antiferromagnetic interaction between the local spin doublets. Most likely, the weak $\pi-\pi$ overlap between adjacent monomeric units along the a axis in compound **3** (see Figure 2) provides the exchange pathway. The position of this maximum is field-dependent and is shifted toward lower temperatures when the field is increased from 0.1 to 4 T (see inset of Figure 7), and it disappears in an applied field of 4 T; the magnetic susceptibility exhibits a plateau at $T < 3$ K for $H \geq 4$ T. These features correspond to a metamagnetic behavior. When the magnitude of the applied magnetic field overcomes the small intrachain antiferromagnetic interaction, the maximum of the magnetic susceptibility disappears, and the magnetic susceptibility tends toward a constant value.

The magnetic properties of compound **3** have been analyzed through the theoretical expression (the Hamiltonian is $\hat{H} = -J\sum_i \hat{S}_i \hat{S}_{i+1}$) proposed by Hall[28] for a uniform chain of local spins $S = 1/2$

(28) Hall, J. W. Ph.D. Dissertation. University of North Carolina, Chapel Hill, NC, 1977.

$$\chi_M = (N\beta^2 g^2/kT)[(0.25 + 0.074975x + 0.075235x^2)/(1 + 0.9931x + 0.172135x^2 + 0.757825x^3)] \quad (1)$$

where N, β, and g have their usual meanings, $x = J/kT$, and J is the exchange coupling constant that describes the magnetic interaction between the two closest-neighbor spin doublets. Such an expression derives from the numerical results from Bonner and Fisher,[29] and it has been normally used to treat the magnetic data of uniform copper(II) chains. The least-squares fit leads to the following parameters: $J = -4.1(1)$ cm^{-1}, $g = 2.10(1)$, and $R = 6.1 \times 10^{-5}$. (R is the agreement factor defined as $\sum_i[(\chi_M)_{obs}(i) - (\chi_M)_{calc}(i)]^2/\sum_i[(\chi_M)_{obs}(i)]^2$.) The curves of the magnetization versus H plot at very low temperatures (see Figure 8) exhibit a crossing point of 4.0 T, which corresponds to the situation in which the magnetic field overcomes the magnetic interaction. The magnitude of the magnetic field at the crossing point provides an evaluation of the magnetic interaction. The exchange coupling constant J would be ca. 4.2 cm^{-1} with $g = 2.10$, a value that agrees with that obtained by the above fit. This example is analogous to that previously reported by some of us for the dicopper(II) complex of formula $[Cu_2(dmphen)_2(dca)_4]$ (dmphen = 2,9-dimethyl-1,10-phenantholine, and dca = dicyanamide), where a very weak magnetic coupling ($J = -3.3$ cm^{-1}) between the two copper(II) ions through the two μ-15-dca bridges occurs.[30]

The magnetic properties of compound **5** in the form of a $\chi_M T$ versus T plot (χ_M is the magnetic susceptibility per two copper(II) ions) are shown in Figure 9. This point is similar to that of the previous compound, but in the present case, no maximum of the magnetic susceptibility was observed in the temperature range explored; the value of $\chi_M T$ at 1.9 K was significantly above that of compound **3** (0.28 cm^3 mol^{-1} K in **5** (per copper atom) versus 0.10 cm^3 mol^{-1} K in compound **3**). These features are consistent with the occurrence of a very small antiferromagnetic interaction in **5** (weaker than that found in **3**). In agreement with the dinuclear structure of compound **5**, we analyze its magnetic data through a simple Bleaney−Bowers expression[31]

$$\chi_M = (2N\beta^2 g^2/kT)[3 + \exp(-J/kT)]^{-1} \quad (2)$$

which is derived through the Hamiltonian $\hat{H} = -J\hat{S}_1\hat{S}_2 + \beta H(g_1\hat{S}_1 + g_2\hat{S}_2)$, where J is the exchange coupling parameter, $S_1 = S_2 = 1/2$ (interacting local spins), $g_1 = g_2 = g$ (average Landé factor), and N, β and k have their usual meanings. The least-squares fit through eq 2 led to the following set of parameters: $J = -0.40(1)$ cm^{-1} and $g = 2.08(1)$ with $R = 8.7 \times 10^{-6}$. (R is the agreement factor defined as $\sum_i[(\chi_M T)_{obs}(i) - (\chi_M T)_{calc}(i)]^2/\sum_i[(\chi_M T)_{obs}(i)]^2$.) The shape of the magnetization versus H plot at 1.9 K is in agreement with the occurrence of a very weak antiferromagnetic interaction; the value of the magnetization at 5 T (the maximum available magnetic filed in our SQUID) is ca. 1.8 μ_B, a value that is somewhat below that expected for two uncoupled spin doublets. The magnetic behavior of compound **5** is practically identical to that previously reported for the parent compound of formula $[Cu_2(N_3)_4(1,3\text{-tpbd})]$.[21]

The magnetic properties of compound **7** in the form of a $\chi_M T$ versus T plot (χ_M is the magnetic susceptibility of two copper(II) ions) are shown in Figure 10. At room temperature, $\chi_M T$ is equal to 0.85 cm^3 mol^{-1} K, a value that is as expected for two magnetically noninteracting spin doublets. Upon cooling, the value of $\chi_M T$ increases, attains maximum at 4.0 K, and then decreases slightly. This behavior is typical of a ferromagnetically coupled dinuclear copper(II) complex; the small decrease in $\chi_M T$ in the low-temperature region is due to zero-field splitting effects (D) and intermolecular interactions. The susceptibility data of compound **7** were analyzed by the corresponding expression[1] for a dicopper(II) unit that is derived through the Hamiltonian for two magnetically interacting local spin doublets derived from the Hamiltonian $\hat{H} = -J\hat{S}_1\hat{S}_2 + \hat{S}_1 D\hat{S}_2 + \beta H(g_1\hat{S}_1 + g_2\hat{S}_2)$, where D is the zero-field splitting of the triplet state. Best-fit results are $J = +8.5(1)$ cm^{-1}, $g = 2.08(1)$, and $|D| = 0.9(2)$ cm^{-1} with $R = 1.6 \times 10^{-5}$. ($\sum_i[(\chi_M T)_{obs}(i) - (\chi_M T)_{calc}(i)]^2/\sum_i[(\chi_M T)_{obs}(i)]^2$.) The theoretical curve matches the experimental values very well over the whole temperature range, as is indicated by the low value of the agreement factor R. It should be noted that the value of D is the maximum value because of the contribution of the intermolecular

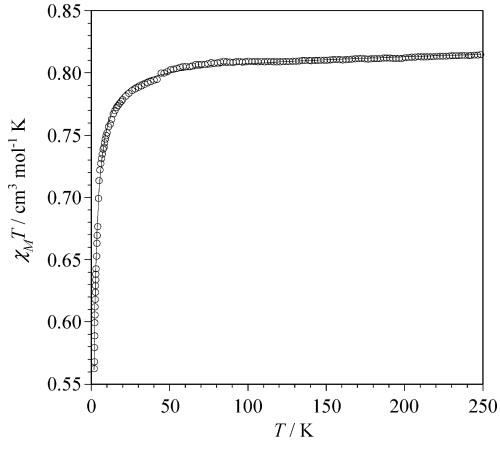

Figure 9. Thermal variation of $\chi_M T$ for compound **5** in an applied magnetic field of 0.1 T including experimental data (○) and a best-fit curve (–) through eq 2. (See the text.)

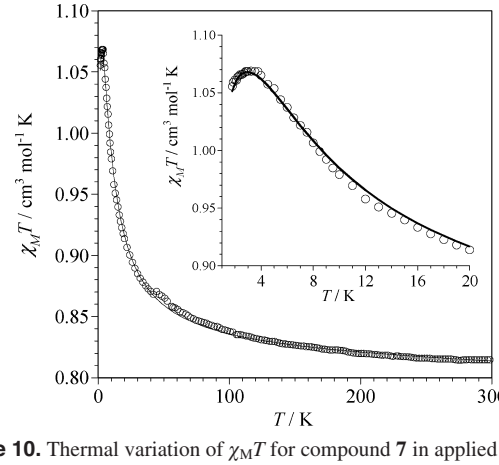

Figure 10. Thermal variation of $\chi_M T$ for compound **7** in applied magnetic fields of 0.1 T ($T \geq 50$ K) and 500 G ($T < 50$ K) including experimental data (○) and a best-fit curve (–) (see the text). The inset shows the maximum of $\chi_M T$ in the low-temperature region.

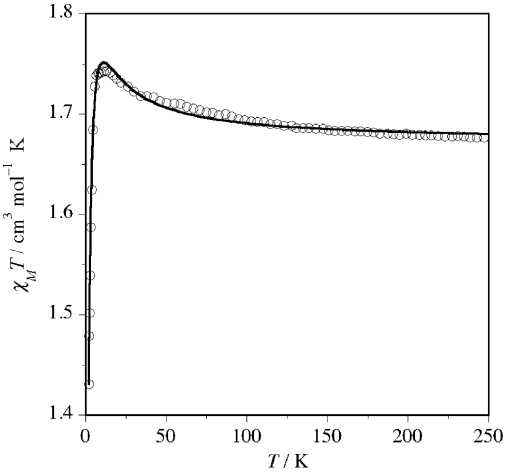

Figure 11. Thermal dependence of $\chi_M T$ for compound **6** including experimental data (○) and a best-fit curve (—). (See the text.)

magnetic interactions that would also occur but that we did not take into consideration. The quality of the fit and the values of J and g remain practically unchanged when the fit is performed with the inclusion of a θ parameter to account for the intermolecular interactions. The fact that the nature and magnitude of the magnetic interaction in **7** is very close to that observed for **1** where the perchlorate bridge is present instead of the dithionate reveals that the exchange pathway is the same in the two dicopper(II) complexes.

The magnetic properties of tetracopper(II) complex **6** in the form of a $\chi_M T$ versus T plot (χ_M is the magnetic susceptibility of four copper(II) ions) are shown in Figure 11. At room temperature, $\chi_M T$ is equal to 1.68 cm^3 mol^{-1} K, a value that is as expected for four magnetically isolated spin doublets (ca. 1.65 cm^3 mol^{-1} K with $g = 2.10$). When cooled, $\chi_M T$ smoothly increases to reach a maximum value of 1.74 cm^3 mol^{-1} K at 4.0 K and further decreases sharply to reach 1.43 cm^3 mol^{-1} K at 1.9 K. These features are consistent with the occurrence of weak ferro- and antiferromagnetic interactions.

Keeping in mind the tetranuclear structure of complex **6**, we analyzed its magnetic data by the Hamiltonian $\hat{H} = -\hat{J}_{13}\hat{S}_1\hat{S}_3 - \hat{J}_{12}\hat{S}_1\hat{S}_2 - \hat{J}_{24}\hat{S}_2\hat{S}_4 + \beta H\,(g_1\hat{S}_1 + g_2\hat{S}_2 + g_3\hat{S}_3 + g_4\hat{S}_4)$, where J_{ij} is the magnetic coupling parameter associated with the interaction between the i and j local spins. To avoid overparametrization in the fitting procedure, we assumed that $g_1 = g_2 = g_3 = g_4 = g$. Regardless, the fit of the magnetic data remains complicated because of the smooth variation of the experimental data and the possible correlation among the four variable parameters. To avoid physically meaningless sets of J_{ij} values in the fitting procedure, theoretical calculations of the DFT type (see Computational Methodology in the Experimental Section) were performed on the dicopper(II) models shown in Figure 12 so that we could visualize and evaluate the efficiency of the intramolecular exchange pathways involved. These models reproduce the three intramolecular exchange pathways in compound **6** (models **I** and **II** for the outer interactions and model **III** for the inner interaction), and their bond distances and angles are those of the real structure.

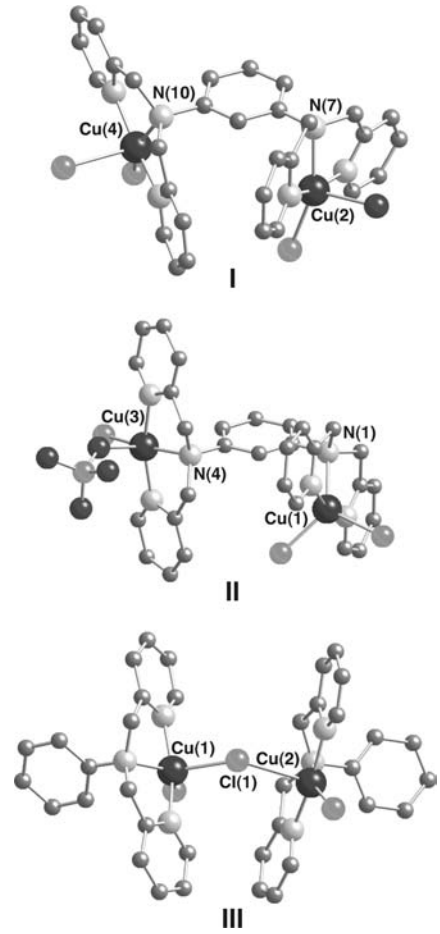

Figure 12. Model systems (**I**−**III**) of the dinuclear copper(II) fragments of compound **6** that were used to perform the DFT-type calculations (see text).

The unpaired electron on each copper(II) ion (that is, the SOMO) in model **I** lies in the basal plane of the metal atom (composed of atoms N(7), N(8), N(9), and Cl(3) for Cu(2) and N(10), N(11), N(12), and Cl(4) for Cu(4)). These two SOMOs are nearly perpendicular to the phenylenediamine plane and lie below this plane. This situation corresponds to the structures of compounds **7** and **1**, where significant and nearly identical ferromagnetic interactions occur (+8.5 and +9.3 cm^{-1} for **7** and **1**, respectively). The theoretical analysis carried out previously for compound **1** accounted for this ferromagnetic interaction.[19] The direct overlap between the $d_{x^2-y^2}$-type magnetic orbitals of the copper atoms and the π system of the pyridyl ligand allows the unpaired spin of the metal to induce a polarization of spin on the bridging skeleton; the alternating spin rule prevails and thus leads to a parallel alignment of the peripheral spins. The calculated value of the magnetic coupling for model **I** (J_{24}) is +30.0 cm^{-1}. Its nature is as predicted, but its value is ca. 3 times that observed in **7** and **1**.

In model **II**, although the SOMO of the Cu(3) atom is also of the $d_{x^2-y^2}$ type (orbital located in the basal plane built by the N(4)N(5)N(6)Cl(5) set of atoms), its orientation is such that it is bisected by the phenylene ring, and the exchange pathway is the σ type. At the other copper atom, Cu(1), the magnetic orbital is of the d_{z^2} type. (The ternary axis roughly corresponds to the N(2)···N(3) vector.) A weak

spin density is expected on the N(1) atom, and the exchange pathway is of the π type at this side. In such a situation, the overlap between the SOMOs of Cu(3) and Cu(1) through the multiatomic Cu(3)−N(4)−C(45)−C(44)−C(43)−N(7)−Cu(2) pathway is expected to be very poor and could be zero by accidental orthogonality. Consequently, the value of the magnetic coupling is expected to be very weak but ferro- or antiferromagnetic in nature.[32,33] The small magnitude of the calculated value of the magnetic coupling for model **II** ($J_{13} = +0.20$ cm^{-1}) fully agrees with this prediction.

Finally, the interacting SOMOs in model **III** are of the d_{z^2} and $d_{x^2-y^2}$ types (at Cu(1) and Cu(2), respectively), as described above. However, in the present case, the exchange pathway is monoatomic, and the bridging atom fills the apical position of the square pyramid at Cu(2) and one equatorial position of the trigonal bipyramid at Cu(1). The orthogonality between the two SOMOs is predicted for such a situation for values of the angle at the bridging chloro (θ) that are close to 180°. Because the value of the Cu(1)−Cl(2)−Cu(2) angle is 141.6(1)°, very weak antiferromagnetic coupling could be expected as a result of the poor overlap between the magnetic orbitals (equatorial−axial exchange pathway; equatorial at Cu(1) and axial at Cu(2)). This conclusion is not supported by the DFT calculations, which afford a calculated value of the magnetic coupling for model **III** of $J_{12} = +11.1$ cm^{-1}.

The fact that the calculated ferromagnetic coupling for model **I** is 3 times the values of the predicted magnetic coupling (that is, the coupling observed for complexes **1** and **7**) and the non-negligible magnetic coupling of model **III** deserves a brief comment. Highly charged molecules or molecules formed by fragments with well-localized charges (i.e., systems that can be considered to be noncovalent) cause problems in the evaluation of the energy and, consequently, of the values of J by methods of computational chemistry. In the present case, it is clear that an overestimation of the ferromagnetic contributions has been derived. Once the ability of the different dinuclear-model fragments to mediate magnetic interactions is evaluated by DFT calculations, we proceed to attempt a fit of the experimental magnetic data on the basis of these results, that is, $|J_{24}| > |J_{13}|$, $|J_{12}| \approx 0$, and $J_{24} > 0$. The analysis of the magnetic data of compound **6** through numerical matrix diagonalization techniques and our use of a Fortran program[34] with the spin Hamiltonian specified above and fixed $J_{12} = 0$ cm^{-1} led to the following set of best-fit parameters: $J_{24} = +8.0$ cm^{-1} and $J_{13} = -3.0$ cm^{-1} and $g = 2.114$ ($R = 1.7 \times 10^{-5}$). These results show that the ferromagnetic coupling between Cu(2) and Cu(4) is ensured, whereas an antiferromagnetic interaction is involved between Cu(1) and Cu(3). To check the influence of the possible intermolecular magnetic interactions on the values of the intramolecular magnetic couplings, a last fit was performed that considered a new parameter accounting for them (θ) and fixed $J_{12} = 0$ cm^{-1}. A better agreement between the experimental and calculated magnetic data is achieved; the best-fit parameters are $J_{24} = +10.4$ cm^{-1} and $J_{13} = -0.4$ cm^{-1}, $\theta = -0.4$ cm^{-1}, and $R = 9.0 \times 10^{-6}$. Now the values of J_{24} and J_{13} fully agree with those observed in the parent complexes **1** and **7** ($J = +9.3$ and $+8.4$ cm^{-1}, respectively) and **5** ($J = -0.40$ cm^{-1}). This is very satisfying because the relative arrangement of the bridging aromatic ring and the magnetic orbitals in complex **5** and model **II** is very close, and the same occurs when comparing model **I** with complexes **1** and **7**. Consequently, we have taken the results of these last fits as the more realistic ones.

Conclusions

A series of copper(II) complexes of the isomeric hexadentate ligands based on phenylenediamine, 1,*n*-tpbd (n = 2−4), has been prepared, and the exchange-polarization mechanism has been successfully tested once more. However, the main aim concerning a thorough comparison of the magnetic properties of stoichiometrically identical, structurally isomeric dicopper(II) complexes of 1,*n*-tpbd without auxiliary bridging ligands still eludes us because of the lack of X-ray-quality crystals of the dinuclear [Cu(1,*n*-tpbd)Cu]$^{4+}$ core as chloride, dithionate, perchlorate, or hexafluorophosphate salts.[20,35] Thus the effect of meta against para versus ortho substitution on the magnetic properties still cannot be assessed satisfactorily in order to test the spin-polarization mechanism. Even though a mononuclear complex of 1,2-tpbd was obtained, the formation of dinuclear complexes can be envisaged given the possibility of different ligand conformations (e.g., a twist around one of the phenylenediamine C−N bonds) and appropriate capping ligands. An optimization of the synthesis of 1,2-tpbd is required before our work can continue with this ligand.

Experimental Section

Materials and Methods. Reagents and solvents used were of commercially available reagent-grade quality. The phenylenediamine ligands were recrystallized prior to use. Ultraviolet−visible spectra were measured on a Hewlett-Packard 8452A or a Shimadzu UV-3100 spectrophotometer. A Bruker AM-300 300-MHz spectrometer was used to record ^{1}H NMR spectra. Infrared spectra were determined on a Mattson Polaris FT-IR spectrometer (Nujol mulls) or as KBr disks by the use of a Hitachi 270-30 IR spectrometer. EI mass spectra were recorded on a Varian MAT311A spectrometer, and FAB mass spectra were recorded on a Kratos MS-50 spectrometer. Elemental analyses were performed at the Chemistry Department II of the Copenhagen University, at Atlantic Microlab, Norcross, Georgia, or at the University of Erlangen. The previously reported procedures were used to prepare *N,N,N′,N′*-tetrakis(2-pyridylmethyl)benzene-1,4-diamine (1,4-tpbd), its copper(II) complexes **2** and $[Cu_2(1,4\text{-tpbd})Cl_4]_n$ (**8**),[20] and *N*-bis(2-pyridylmethyl)benzeneamine (phbpa).[22]

(29) Bonner, J. C.; Fisher, M. E. *Phys. Rev. A* **1964**, *135*, 640–658.
(30) Carranza, J.; Sletten, J.; Lloret, F.; Julve, M. *Inorg. Chim. Acta* **2004**, *357*, 3304–3316.
(31) Bleaney, B.; Bowers, K. D. *Proc. R. Soc. London, Ser. A* **1952**, *214*, 451–465.
(32) Felthouse, T. R.; Duesler, E. N.; Hendrickson, D. N. *J. Am. Chem. Soc.* **1978**, *100*, 618–619.
(33) Felthouse, T. R.; Hendrickson, D. N. *Inorg. Chem.* **1978**, *17*, 2636–2648.
(34) Cano, J. *VPMAG Package*; University of Valencia: Valencia, 2003.
(35) Schindler, S.; Szalda, D. J.; Creutz, C. *Inorg. Chem.* **1992**, *31*, 2255–2264.

Caution! *Perchlorate salts are potentially explosive, and they should be handled with care. Our preparations were carried out on a millimole scale, and heating was avoided.*

Preparation of the Ligands and Complexes. *N,N,N′,N′*-Tetrakis(2-pyridylmethyl)benzene-1,3-diamine (1,3-tpbd). The synthesis of 1,3-tpbd was performed as described earlier[35] but could be improved by the use of an excess of 2-chloromethylpyridine hydrochloride (molar ratio of chloromethylpyridine to 1,3-phenylenediamine is 1:5). In contrast with the previously published synthesis, one recrystallization from acetone with a small amount of active charcoal was sufficient to purify the crude product, and no trace of the trisubstituted phenylenediamine, *N,N,N′*-tris(2-pyridylmethyl)benzene-1,3-diamine, was detected. The analytical data are the same as those reported earlier, but the yield was increased to 70% (to be compared with 25% obtained previously).

Dichlorido[*N*-bis(2-pyridylmethyl)benzeneamine]copper(II), [$CuCl_2$(phbpa)] (3). A mixture of $CuCl_2 \cdot 2H_2O$ (31 mg, 0.1818 mmol) in 2 mL of methanol was added to a methanolic solution (5 mL) of phbpa (50 mg, 0.1818 mmol). The product precipitates as light-green needles after 2 days. Yield: 50.1 mg, 67.3%. Anal. Calcd for $C_{18}H_{17}Cl_2CuN_3$: C, 52.76; H, 4.18; N, 10.25. Found: C, 52.57; H, 4.24; N, 10.14. FAB−MS *m*/*z*: 373 ([CuCl(phbpa)]$^+$, 100%), 338 ([Cu(phbpa)]$^{2+}$, 55%). UV−vis (MeOH) λ, nm (ε, dm^3 mol^{-1} cm^{-1}): 258 (13 161), 306 (2238), 378 (sh, 404), 702 (187).

(Tetrakis-*N,N,N′,N′*-(2-pyridylmethyl)-1,2-benzenediamine)copper(II) dihexafluorophosphate dihydrate, [Cu(1,2-tpbd)]$(PF_6)_2 \cdot 2H_2O$ (4). Picolyl chloride hydrochloride (3.8 g, 23.11 mmol) and *o*-phenylenediamine (0.5 g, 4.63 mmol) were dissolved in water (10 mL) under an argon atmosphere. Sodium hydroxide (0.925 g, 23.11 mmol) in a minimum amount of water was added over a period of 2 h. The pH was kept at 9.0 during the next 7−10 days by the occasional addition of NaOH (in all, 0.740 g, 18.45 mmol) in 7 mL of water. The solution was extracted with 30 mL of CH_2Cl_2 five times, and the combined organic phases were dried over Na_2SO_4. The evaporation of the solvent yielded a yellow oil, which contained the desired ligand, tetrakis-*N,N,N′,N′*-(2-pyridylmethyl)-1,2-benzenediamine (1,2-tpbd), and the major byproduct, tri-*N,N,N′*-(2-pyridylmethyl)-1,2-benzenediamine. Complex formation was achieved by reacting this mixture (ca. 0.1 mmol in 1,2-tpbd based on NMR integrations) with $Cu(NO_3)_2 \cdot 5H_2O$ (0.1 mmol) and a further addition of NH_4PF_6 (0.5 mmol) in MeOH (5 mL). Overnight, [Cu(1,2-tpbd)]$(PF_6)_2 \cdot 2H_2O$ was deposited as blue crystals in variable yields. Found: C, 41.67; H 3.27; N, 9.82. $C_{30}H_{32}CuF_{12}N_6O_2P_2$ requires C, 41.79; H, 3.74; N, 9.75.

Tetrachlorido[*N,N,N′,N′*-tetrakis(2-pyridylmethyl)benzene-1,3-diamine]dicopper(II), $[Cu_2Cl_4$(1,3-tpbd)$] \cdot H_2O \cdot CH_3OH$ (5). A mixture of $CuCl_2 \cdot 2H_2O$ (0.36 g, 2.1 mmol) dissolved in 10 mL of water was added to a suspension of 1,3-tpbd (0.5 g, 1 mmol) in 10 mL of methanol. After 10 min of stirring, the solution was filtered and was left to stand overnight. The green crystals deposited were filtered and dried in air. Yield: 0.4 g, 50.5%. Anal. Calcd for $C_{31}H_{34}N_6Cu_2O_2Cl_4 \cdot H_2O \cdot CH_3OH$ (**5**): C, 47.04; H, 4.33; N, 10.62. Found: C, 47.05; H, 4.13; N, 10.82. UV−vis (MeOH) λ, nm (ε, dm^3 mol^{-1} cm^{-1}): 375 (sh, 702), 726 (268).

***μ*-Chlorido-bis[dichlorido-perchlorato-(*N,N,N′,N′*-tetrakis(2-pyridylmethyl)benzene-1,3-diamine)dicopper(II)]diperchlorate-[$(Cu_2Cl_2(ClO_4)$(1,3-tpbd))$Cl(Cu_2Cl_2(OH_2)$(1,3-tpbd))$](ClO_4)_2$ (6).** A mixture of $CuCl_2 \cdot 2H_2O$ (0.11 g, 0.63 mmol) and $Cu(ClO_4)_2 \cdot 6H_2O$ (0.23 g, 0.63 mmol) dissolved in 15 mL of water was added to a suspension of 1,3-tpbd (0.3 g, 0.63 mmol) in 15 mL of methanol. After 10 min of stirring, the solution was filtered and left to stand for a few days. The green crystals deposited were filtered and dried in air. Yield: 0.4 g, 50.5%. Found: C, 42.70; H, 3.34; N, 9.86. $C_{60}H_{56}N_{12}Cu_4O_{13}Cl_8$ requires C, 42.62; H, 3.34; N, 9.94. UV−vis (MeOH) λ, nm (ε, dm^3 mol^{-1} cm^{-1}): 375 (sh, 702), 726 (268).

Diaqua[*N,N,N′,N′*-tetrakis(2-pyridylmethyl)benzene-1,3-diamine]dicopper(II) dithionate, $[Cu_2(OH_2)_2(S_2O_6)$(1,3-tpbd)$]S_2O_6 \cdot 3H_2O \cdot CH_3OH$) (7). A mixture of $Cu(BF_4)_2 \cdot 6H_2O$ (0.44 g, 1.26 mmol) dissolved in 15 mL of water was added to a suspension of 1,3-tpbd (0.3 g, 0.63 mmol) in 15 mL of methanol. A mixture of $Na_2S_2O_6$ (1 g, 4.13 mmol) in 50 mL of water was added, and the solution was filtered after boiling for a few minutes. The green crystals that deposited overnight were filtered off and dried in air. Yield: 0.4 g, 62.2%. Anal. Calcd for $C_{31}H_{42}Cu_2N_6O_{18}S_4$ (**7**): C, 35.73; H, 4.06; N, 8.06. Found: C, 35.16; H, 3.83; N, 8.23.

Magnetic Measurements. Magnetic susceptibility data of polycrystalline samples of compounds **3** and **5**−**7** were collected over the temperature range of 1.9−300 K with a Quantum Design SQUID susceptometer and by the use of applied magnetic fields of 0.1 T (compounds **3** and **5**−**7**) and 500 G (compounds **6** and **7**). Magnetization isotherms ($1.85 \leq T \leq 3.5$) varying the applied magnetic field in the range of 0−5 T were performed for compound **3**. Diamagnetic corrections for the constituent atoms and corrections for the sample holder were performed. The correction for the temperature-independent paramagnetism (60×10^{-6} cm^3 mol^{-1} per copper(II) ion) was also applied.

Computational Methodology. The computational strategy used in this work has been described elsewhere, and it is briefly outlined here.[36] For the evaluation of the coupling constant for each dicopper(II) model fragment of compound **6** (models **I**−**III**, Figure 12), two separate calculations were carried out using DFT, one for the triplet state and another one for the low-spin, broken-symmetry state. The hybrid B3LYP method[37] was used in the calculations as implemented in Gaussian 98,[37] and the all-electron double-ζ basis proposed by Ahlrichs and coworkers was used, except for copper, where we have used a triple-ζ basis.[38] The real dinuclear fragments of compound **6** were used in the calculations to estimate the values of the intramolecular magnetic couplings.

X-ray Crystallography. Single crystals were obtained directly from reaction mixtures. Because of the solvent loss, crystals of compounds **4**, **5**, and **7** used for structural analysis show slightly different lattice-solvent compositions than those found in the elemental analysis. Data were collected on a Huber four-circle diffractometer (for compound **3**) and on a Siemens SMART diffractometer[39] for the other structures. Crystal data and experimental parameters are presented in Table 1. The crystallographic data were deposited as supplementary publication no. CCDC-674771−674773 for compounds **3**−**5**, CCDC-676829 for compound **6**, and CCDC-676828 for compound **7** at the Cambridge Crystallographic Data Centre and can be obtained, on request, from the director, Cambridge Crystallographic Data Centre, 12 Union Road, Cambridge, CB2 1EZ, U.K. (Fax: (+44)1223-336-033. E-mail: deposit@ccdc.cam.ac.uk)). The data were corrected for Lorentz-polarization effects, and absorption corrections were made by an integration for compounds **3** and **6** and by SADABS,[40] a multiscan technique, for compounds **4**, **5**, and **7**. The structures

(36) Ruiz, E.; Alemany, P.; Alvarez, S.; Cano, J. *J. Am. Chem. Soc.* **1997**, *119*, 1297–1303.
(37) Becke, A. D. *J. Chem. Phys.* **1993**, *98*, 5648–5652.
(38) Schäfer, A.; Horn, H.; Ahlrichs, R. *J. Chem. Phys.* **1992**, *97*, 2571–2577.
(39) *SMART, SAINT, and XPREP Area-Detector Control Integration Software*; Siemens Analytical X-ray Instruments: Madison, WI, 1995.
(40) *SADABS*, 2.26; Bruker AXS: Madison, WI, 2002.

were solved by direct methods, SHELX[41] for compound **7**·$2H_2O$·CH_3OH and SIR97[42] for compounds **3**, **4**, and **5**·$0.84CH_3OH$, and were refined by least-squares techniques using programs from SHELX[41] or from KRYSTAL.[43] Atomic-scattering factors were taken from ref 44 for compound **7** and from ref 45 for the other structures. All non-hydrogen atoms for compound **3** were refined anisotropically (on *F*), whereas the hydrogen atoms were refined isotropically. All non-hydrogen atoms for compound **5**·$0.84CH_3OH$ were also anisotropically refined (on *F*), whereas the hydrogen atoms of the ligand were placed in fixed calculated positions (C−H = 0.95 Å). The molecules of methanol are disordered over two sites with occupancy factors of 0.53(1) and 0.31(1), and their hydrogen atoms were not included in the calculations. All non-hydrogen atoms for compound **7**·$2H_2O$·CH_3OH were refined anisotropically (on F^2). The hydrogen atoms of the water molecule in this compound were refined isotropically, whereas C−H distances were kept fixed (C−H = 0.97 and 0.93 Å for aliphatic and aromatic carbon atoms, respectively). The hydrogen atoms of the disordered methanol molecules were not included in the calculations. The absolute structure parameter[46] was 0.005(5), which indicates that the correct polarity has been chosen. All non-hydrogen atoms for compound **4** were refined anisotropically (on *F*), and the hydrogen atoms of the ligands were kept fixed in calculated positions (C−H = 0.95 Å).

Acknowledgment. S. Schindler acknowledges financial support from the Deutsche Forschungsgemeinschaft and from Professor Hans Toftlund (University of Southern Denmark). Support from the Danish Natural Science Research Council is acknowledged by C. J. McKenzie. A. Hazell thanks the Carlsberg Foundation for the diffractometers. J. Cano thanks the Universitat de València for a grant as an invited Professor. Furthermore, we thank Jens Zacho Pedersen and Hans Toftlund (University of Southern Denmark) for their assistance. We also thank the Ministerio Español de Ciencia y Tecnología and to the Comissió Interdepartamental de Ciència i Tecnologia (CIRIT) for financial support through projects CTQ2007-61690 and CTQ2005-08123-C02-02/BQU and 2005SGR-00036.

IC800244G

(41) Sheldrick, G. M. *SHELX-97*; Universität Göttingen: Göttingen, Germany, 1997.
(42) Altomare, A.; Cascarano, G.; Giacovazzo, C.; Guagliardi, A.; Moliterni, A. G. G.; Burla, M. C.; Polidori, G.; Camalli, M.; Spagna, R. *SIR97*; Universities of Bari, Perugia, and Roma: Italy, 1997.
(43) Hazell, A. *KRYSTAL*; Aarhus University: Denmark, 1995.
(44) *International Tables for X-RAY Crystallography*; Kynoch Press: Birmingham, England, 1992.
(45) *International Tables for X-RAY Crystallography*; Kynoch Press: Birmingham, England, 1974.
(46) Flack, H. D. *Acta Crystallogr., Sect. A* **1983**, *39*, 876–881.